

Orbits and masses in two triple systems

Dinko Nazor¹^{*} and Andrei Tokovinin²[†]

¹ Pixel Ribs d.o.o. - Vlačka 79, 10000 Zagreb, Croatia

² Cerro Tololo Inter-American Observatory – NSF’s NOIRLab, Casilla 603, La Serena, Chile

ABSTRACT

In an effort to determine accurate orbital and physical properties of a large number of bright stars, a method was developed to fit simultaneously stellar parameters (masses, luminosities, effective temperatures), distance, and orbits to the available data on multiple systems, namely the combined and differential photometry, positional measurements, radial velocities (RVs), accelerations, etc. The method is applied to a peculiar resolved triple system HIP 86286. The masses of its components estimated using observations and standard relations are 1.3, 0.9, and 0.9 M_{\odot} ; the main star is a G8IV subgiant, while its two companions are main-sequence dwarfs. The inner and outer orbital periods are 35 and 287 years, respectively, and the orbits are nearly coplanar. The second system, HIP 117258, is an accelerating star with a resolved companion; its 35.7-yr orbit based on relative astrometry and precise RVs yields the secondary mass of 0.95 M_{\odot} , much larger than inferred from the photometry. The apparent paradox is explained by assuming that the secondary is a close pair of M-type dwarfs with yet unknown period.

Key words: binaries: visual – binaries: spectroscopic – stars: individual: HIP 86286 – stars: individual: HIP 117258

1 INTRODUCTION

Astronomy is based on observations, and this general statement is fully relevant for the study of stellar multiple systems. Only the brightest stars were accessible to visual examination or photographic spectroscopy in the 19th century. As the astronomical technology progressed, larger samples of fainter objects became scrutinized. The Tycho mission on board the Hipparcos satellite examined all sky down to the 12th magnitude. Its combination with prior ground-based astrometry resulted in the Tycho-2 catalogue of 2.5 million stars with accurate positions and proper motions (PMs) (Høg et al. 2000). Nowadays, the Gaia project pushes the limits much further by monitoring billions of stars down to the 21st magnitude (Gaia Collaboration 2021). For the brighter part of the Gaia targets, astrometry is complemented by spectroscopy. The number of astrometric and spectroscopic orbits published in the Gaia catalogue of non-single stars (Gaia Collaboration 2023) already surpasses the totality of previously known ground-based orbits, although the latter cover a much wider range of periods.

Despite this tremendous progress, the brightest stars still possess the most detailed and complete observations. Furthermore, many systems of two or more stars have problematic data in Gaia for various reasons. In an effort to assemble the most up-to-date and accurate data on the stars of the Tycho catalogue, numerous cases of missing or unsatisfactory data were identified. This prompted detailed examination of observed motions in selected multiple systems and determination or update of their orbits. The purpose of this paper is to share several results of this work undertaken by the first author (DN), a programmer and an amateur astronomer. The role of the co-

author (AT) is to verify the results and to present them in a concise way, contributing professional experience to this collaboration.

In the epoch of large surveys, individual examination of multiple systems might appear outdated. Yet, most (if not all) surveys are designed for single stars; the presence of one or several additional components affects the single-star pipelines and leads to biases and errors, sometimes significant. For example, 2/3 binary stars with known visual orbits still lack Gaia parallaxes (Chulkov & Malkov 2022). With the planned 11 yr duration of the full Gaia mission, orbits with longer periods have to rely on the complementary ground-based observations.

The methods of orbit calculation and assessment of stellar parameters are briefly outlined in Section 2. Then in Section 3 one interesting resolved triple system is studied in detail to illustrate this approach. Section 4 reveals another unusual case, namely a hidden triple where the dim secondary is in fact a close pair of low-mass stars. The paper is summarized in Section 5.

2 DATA AND METHODS

As a part of a greater effort to validate and improve existing orbits and compute new ones, DN has written a framework of classes and functions. The language of choice is C/C++ for its well-known high performance. The main goal is to come up with a unified, robust, and dynamic model of our Galactic neighbourhood. There is no “ready-to-use” application where the input is dropped-in and results are spat-out. Each case rather needs to be individually programmed. This may seem like a drawback, but the reality is that many systems require a particular intervention that wouldn’t be possible with a ready-to-use software and without some fine-tuning. So, when such

* E-mail: dinko.nazor@gmail.com

† E-mail: andrei.tokovinin@noirlab.edu

situation is encountered, usually a small adaptation can make a big difference.

The general types of models that the framework supports are 2 to 4-star systems in A-B, Aab-B, A-Bab, and Aab-Bab configurations. The accepted input data are relative positions, RVs, accelerations, light-source “wobbling”, light curves, times of minima for eclipsing binaries, and observed magnitudes in the $U, B, V, R, I, J, H, K, G, G_{BP}, G_{RP}, u, g, r, i, z$ bands. The model represents orbits, astrometry, and stellar parameters of each star in over 60-dimensional parameter space. It is highly optimized for performance, so for example, for systems with more than two components, the light-time effect can be enabled and taken into account with negligible additional computational cost. Quadratic limb darkening coefficients for computing magnitudes during eclipses are implemented using the tables from Claret (2018) to get the coefficients for a particular star from its effective temperature and gravity. The model is also very versatile. For example, it allows different system velocities to be assigned to multiple sets of RVs. Rectilinear solution is the last resort for wide binaries for which the observed relative motion has a short time coverage or has not exhibited sufficient changes.

For computing stellar parameters, DN has implemented various models for different types of stars. The tables from Pecaute & Mamajek (2013), updated online,¹ have proven to be the best choice; for red stars with $T_{\text{eff}} < 5500\text{K}$, the 2019 version of the online tables gives slightly better results than the 2021 version. The BT-Settl (Baraffe et al. 2015) and PARSEC (Bressan et al. 2012) evolutionary tracks are used for evolved stars. Please, note that stellar masses and other parameters derived here are model-dependent. Our goal is to find the best set of self-consistent parameters that fits the available data, rather than to test stellar evolutionary models.

As usual, the solvers try to find the global minimum of χ^2 . The core solver is based on the Gauss-Newton method with Moore-Penrose inverse, with a custom line-search algorithm. It is a numerical method which finds the local χ^2 minimum, given an initial guess, down to the 64-bit precision of floating-point numbers.

The initial guess can be either found by a combination of MCMC (Foreman-Mackey et al. 2013) and simulated annealing, or it can simply be (in most cases) a known (good) solution. In the former case, several different attempts are constructed and manually inspected to verify similarity of the convergences. The parameters can be fixed or ignored during computation (the algorithm automatically recognizes parameters that are not affected by the input data and disables them), and any additional specific constraints can be added easily via lambda functions. Automatic computation of parameters can also be included in the process via lambda functions (e.g. when radii are fixed to fill stars’ Roche lobes, when the mass-radius relationship is for some reason strictly determined, or when limb darkening coefficients are computed from the stellar parameters). The Gauss-Newton solver might fail if the inputs are “too contradictory” or if the solution is not well constrained or defined. To get around this problem, a simple manual data reduction or assigning smaller weights to outliers are helpful. The solver is rather fast; it converges within a few 10th of a second (less than 100 iterations) even with hundreds of positions or thousands of light-curve measurements, for example.

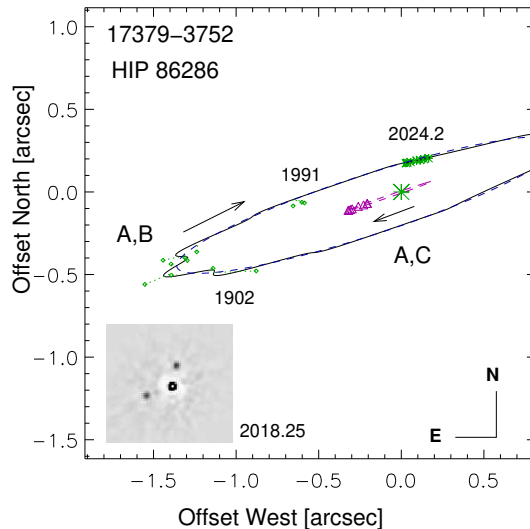


Figure 1. Orbits of the triple system HIP 86286 (axis scale in arcseconds). The magenta triangles and ellipse show the measured positions and the orbit of the inner subsystem A,C. The black solid line depicts the outer orbit with wobble caused by the subsystem, while the blue dashed line is the outer orbit without wobble. Positions of the outer pair are plotted as small green crosses and larger green asterisks when they correspond to AC,B and A,B, respectively. The insert shows the shift-and-add image taken at SOAR on 2018.25 and indicating true quadrants of the companions.

3 THE TRIPLE SYSTEM HIP 86286 (GJ 683.2)

This bright stellar system, known as HIP 86286, HD 159704, WDS J17379-3752, and GJ 683.2, was resolved in 1897 by R. Innes as a $1''$ pair; it bears the discoverer name I 247. The separation between A and its faint companion B gradually decreased during the 20th century. This neglected pair was observed by the speckle camera at the 4.1 m Southern Astrophysical Research (SOAR) telescope in 2017 at the request by R. Gould and found to be a resolved triple with two companions B and C of comparable brightness and at comparable separations (Tokovinin et al. 2018). Such trapezium-type configurations are expected to be dynamically unstable. The perplexing “triangular” system was re-visited at SOAR with a yearly cadence, revealing slow motion of both companions in opposite directions (C is receding from A and B is approaching). AT suspected initially that one of the companions could be unrelated (the sky in this region is crowded). However, in such a case the fast PM of $(-5.2, -131.5) \text{ mas yr}^{-1}$ (van Leeuwen 2007) would have changed the configuration rapidly, so both companions are actually physically bound to A.

In June 2021, DN stumbled upon this interesting system while revising information on Tycho stars. He noted the strange triangular configuration with comparable separations and also concluded that companions B and C are related to A. Assuming initially that the companion C was unrelated, he tried to compute the orbit of AB, but it matched the measured positions very poorly. There was also a significant discrepancy between the Hipparcos and Gaia DR2 PMs; the acceleration computed from the provisional AB orbit could not possibly explain the measured one of the primary. It clearly suggested that the primary should be accelerating in the opposite direction! The only explanation was the reflex motion of A in the inner orbit AC.

A model for three-star system was set up and fed with the data. Due to the shortness of the observed arcs and unavailability of other data (RVs), the solution was still purely for demonstrative purposes.

¹ https://www.pas.rochester.edu/~emama-jek/EEM_dwarf_UBVIJHK_colors_Teff.txt

emama-

Table 1. Orbits and Astrometry of HIP 86286

| Element | A,C | AC,B |
|--|--------------------------------|--------------------|
| P (yr) | 34.95 ± 0.05 | 287.0 ± 1.4 |
| T (JY) | 2041.907 ± 0.022 | 2049.65 ± 0.40 |
| e | 0.270 ± 0.022 | 0.192 ± 0.005 |
| a (″) | 0.2677 | 1.2204 |
| Ω (deg) | 109.05 ± 0.20 | 107.86 ± 0.22 |
| ω (deg) | 180.77 ± 0.22 | 156.58 ± 0.22 |
| i (deg) | 88.54 ± 0.22 | 98.69 ± 0.07 |
| RA, Decl. (J2000) | 17:37:51.2284, $-37:51:41.053$ | |
| $\mu_{\alpha}^*, \mu_{\delta}$ (mas yr $^{-1}$) | $-10.52, -129.52$ | |
| Parallax (mas) | 19.274 ± 0.041 | |

Table 2. Stellar Parameters and Photometry of HIP 86286

| Parameter | A | C | B | A+B+C |
|--------------------------|--------|-------|-------|--------------|
| Mass (M_{\odot}) | 1.28 | 0.91 | 0.89 | 3.08 |
| Radius (R_{\odot}) | 2.27 | 0.89 | 0.86 | – |
| T_{eff} (K) | 5421 | 5451 | 5370 | – |
| L (L_{\odot}) | 4.01 | 0.624 | 0.552 | – |
| $\log g$ (cm s $^{-2}$) | 3.83 | 4.50 | 4.52 | – |
| Sp. Type | G8.5IV | G8.3V | G8.8V | – |
| B (mag) | 7.717 | 9.749 | 9.927 | 7.45 (7.45) |
| V (mag) | 6.959 | 9.007 | 9.161 | 6.69 (6.68) |
| R_C (mag) | 6.542 | 8.598 | 8.742 | 6.27 (6.28) |
| I_C (mag) | 6.151 | 8.212 | 8.742 | 5.88 (5.88) |
| J (mag) | 5.578 | 7.646 | 7.765 | 5.31 (5.36:) |
| H (mag) | 5.224 | 7.298 | 7.405 | 4.95 (5.12:) |
| K_s (mag) | 5.141 | 7.215 | 7.319 | 4.87 (4.87) |
| G (mag) | 6.752 | 8.815 | 8.960 | 6.48 (6.48) |
| G_{BP} (mag) | 7.156 | 9.222 | 9.381 | 6.89 (6.90) |
| G_{RP} (mag) | 6.221 | 8.309 | 8.442 | 5.96 (5.95) |

However, all relative positions could be closely matched and the strange motion of the primary star A was reproduced well, within the assumed errors. So, the object has revealed itself beyond any doubt as a triple system: a close binary AC with a period of a few decades and their outer companion B in a few hundred year orbit. Star A is an evolved subgiant and both companions are lighter and assumed to still be on the main sequence.

At this point, the information was shared with AT who confirmed the validity of the proposed triple-star model. A preliminary version of these orbits is listed in the online Multiple Star catalogue (Tokovinin 2018). The orbits are determined here using the latest (up to 2024.2) position measurements at SOAR. The inner and outer orbits are plotted in Fig. 1. The orbital elements, position, and motion of the centre of mass are listed in Table 1, while stellar parameters are given in Table 2. They were determined by the joint fit to positions and photometry, as explained below.

The input data include the combined photometry in bands from B to K_s (the measurements are given in brackets in the last column of Table 2). The errors of 0.1 mag are assumed, and the uncertain 2MASS photometry in the J and H bands is not used. The model reproduces the combined photometry very well. The model also uses the differential photometry from SOAR in the I_C band: $\Delta m_{AC} = 2.06 \pm 0.10$ mag, $\Delta m_{AB} = 2.19 \pm 0.10$ mag. The Gaia photometry is taken from DR2. Zero interstellar extinction is adopted, considering the small distance, and confirmed during preliminary computations. Table 3 lists the position measurements, residuals from the

Table 3. Positions and residuals of HIP 86286

| Date (JY) | θ_{2000} (deg) | (O-C) $_{\theta}$ (deg) | σ_{θ} (deg) | ρ (mas) | (O-C) $_{\rho}$ (mas) | σ_{ρ} (mas) |
|----------------------|-----------------------|-------------------------|-------------------------|--------------|-----------------------|-----------------------|
| AC (inner pair) | | | | | | |
| 2017.5345 | 108.6 | −0.0 | 0.5 | 216.9 | −0.3 | 2.0 |
| 2017.5345 | 108.7 | 0.1 | 999.9 | 219.1 | 1.9 | 99.9 |
| 2018.2526 | 108.9 | 0.2 | 0.5 | 241.7 | 0.3 | 2.0 |
| 2019.3803 | 108.5 | −0.3 | 0.5 | 274.5 | 0.3 | 2.0 |
| 2021.2452 | 108.9 | 0.0 | 0.5 | 314.6 | 0.3 | 2.0 |
| 2022.1954 | 109.0 | 0.1 | 0.5 | 326.4 | −1.2 | 2.0 |
| 2023.3243 | 109.0 | 0.0 | 0.5 | 337.2 | 0.0 | 2.0 |
| 2024.2391 | 109.0 | −0.0 | 0.5 | 340.4 | 0.5 | 2.0 |
| AC-B (unresolved AC) | | | | | | |
| 1897.0009 | 119.3 | 6.1 | 999.9 | 1000.0 | −234.1 | 500.0 |
| 1902.4308 | 112.1 | −0.2 | 1.5 | 1230.0 | −17.5 | 50.0 |
| 1914.6205 | 109.9 | −0.4 | 1.5 | 1480.0 | 4.2 | 50.0 |
| 1920.5604 | 109.8 | 0.3 | 1.5 | 1650.0 | 132.1 | 200.0 |
| 1929.6102 | 107.4 | −0.9 | 1.5 | 1460.0 | 6.0 | 50.0 |
| 1936.4801 | 106.9 | −0.4 | 1.5 | 1370.0 | 9.0 | 50.0 |
| 1938.8400 | 107.8 | 0.8 | 1.5 | 1360.0 | 1.8 | 50.0 |
| 1943.2499 | 106.0 | −0.4 | 1.5 | 1500.0 | 110.7 | 300.0 |
| 1959.6196 | 106.3 | 2.2 | 3.0 | 1290.0 | −5.2 | 50.0 |
| 1991.1889 | 97.3 | 2.6 | 3.0 | 660.0 | −30.4 | 50.0 |
| 1991.2500 | 96.0 | 3.5 | 10.0 | 605.0 | 7.9 | 100.0 |
| 1991.5700 | 96.5 | 4.3 | 10.0 | 590.0 | 0.8 | 100.0 |
| A-B (resolved AC) | | | | | | |
| 2017.5345 | 350.8 | −0.3 | 0.5 | 176.3 | −0.4 | 2.5 |
| 2017.5345 | 351.8 | 0.7 | 999.9 | 176.1 | −0.6 | 99.9 |
| 2018.2526 | 348.1 | 0.3 | 0.5 | 180.2 | −0.4 | 2.5 |
| 2019.3803 | 342.7 | 0.1 | 0.5 | 189.4 | 0.4 | 2.5 |
| 2021.2452 | 334.0 | 0.2 | 0.5 | 210.7 | 1.2 | 2.5 |
| 2022.1954 | 329.5 | −0.0 | 0.5 | 224.1 | 0.6 | 2.5 |
| 2023.3243 | 324.9 | 0.1 | 0.5 | 241.8 | −1.5 | 2.5 |
| 2024.2391 | 320.9 | −0.4 | 0.5 | 262.5 | 0.5 | 2.5 |

orbits, and adopted errors. The position angles θ are corrected for precession to the epoch 2000.0, the separations ρ are given in mas. The published measurements at SOAR in 2017–2020 are corrected for minor systematic errors as prescribed in (Tokovinin et al. 2022). Large errors are assigned to the inaccurate positions, effectively canceling these data. Visual measurements of AB-C made before 1991 were retrieved from the Washington Double Stars (WDS) database, the measurements in 1991 come from the Hipparcos and Tycho missions, and the remaining data are obtained at SOAR. Note that the companion’s designations B and C are swapped in the published SOAR data.

The errors of the orbital elements are determined by running the MCMC chains 10^4 times and fitting Gaussians to the distributions of the resulting elements, which are nicely bell-shaped. However, the explored region of the parameter space was restricted by the condition $\chi^2 < \chi^2_{\text{min}} + 5$. The MCMC did not return any χ^2 smaller than the minimum χ^2_{min} found by the Gauss-Newton method. The semimajor axis was not among the fitted parameters (it is computed from the masses, periods, and parallax), so its errors are not given in Table 1. AT checked the results with the IDL code `orbit3` that fits only the orbital elements (Tokovinin 2017). Similar elements, but with much larger errors, were found. So, the errors in Table 1 might be underestimated.

Stellar parameters of the main-sequence stars B and C are derived from the online tables of Mamajek (2019 version), while the magnitudes of the evolved star A are modeled according to the 2021

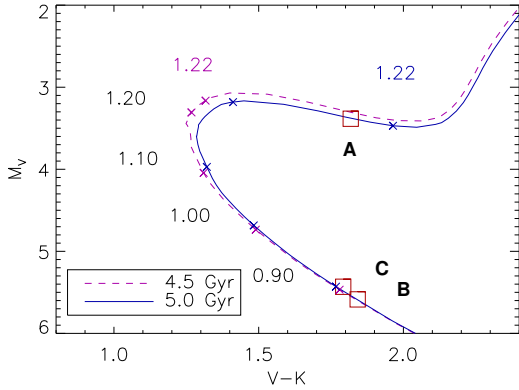


Figure 2. Colour-magnitude diagram of the triple system HIP 86286 (squares) and PARSEC isochrones for 4.5 Gyr and 5 Gyr and solar metallicity, with masses marked. The mass of A estimated from the isochrones is $1.22 M_{\odot}$.

version of these tables. The masses M of dwarfs and subgiants with $M > 0.8 M_{\odot}$ are computed from effective temperature T_{eff} and luminosity L by the formula 19 from [Montalto et al. \(2021\)](#), based on Table 10 of [Moya et al. \(2018\)](#):

$$\log(M/M_{\odot}) = -0.119 + 2.14 \cdot 10^{-5} T_{\text{eff}} + 0.1837 \log(L/L_{\odot}). \quad (1)$$

We preferred to use this formula (rather than tables) because the evolutionary tracks are not monotonous, precluding convergence in some cases. For dwarfs less massive than $0.8 M_{\odot}$, we use instead the 5th order polynomial from [Mann et al. \(2019\)](#) relating mass to the absolute magnitude M_{K_s} . The code fits simultaneously orbits, effective temperatures T_{eff} , radii R of all components, and the parallax. For a given pair of T_{eff} , R values, the luminosities and masses are computed; the gravity $\log g$ is derived from M and R . Using the bolometric corrections and colours given by the standard relations, the absolute magnitudes in different photometric bands are determined. They are translated into actual magnitudes by adding the distance modulus and extinction and fitted to the available combined and differential photometry. For single stars, the parameters derived by this method are very close to those found in the TESS Input Catalogue ([Stassun et al. 2019](#)). The third Kepler law is built into the model, so the semimajor axis of each orbit is computed from its period, mass sum, and parallax.

Our model determines the parallax of 19.274 mas, so the star is definitely beyond the 25 pc limit of the Gliese catalogue of nearby stars (it was likely included there because of the large photometric parallax and a fast PM). The space astrometry of this triple system is discordant: Hipparcos measured a parallax of 21.02 ± 1.09 mas ([van Leeuwen 2007](#)), Gaia DR2 — 16.33 ± 0.46 mas, and Gaia DR3 — 14.71 ± 0.80 mas. The large RUWE of 20.5 and the bias of the parallax in Gaia are likely produced by displacements of the photocentre due to the unresolved companions C and B. This shift depends on the scan direction, which changes regularly during the year, biasing eventually the parallax. This source is challenging for Gaia, and even the final data release might fail to give good results, unless a triple-star model is fitted explicitly.

The PM of the system derived from its positions in the Hipparcos and Gaia DR3 catalogues is $(\mu_{\alpha}^*, \mu_{\delta}) = (-10.517, -129.521)$ mas yr $^{-1}$ ([Brandt 2021](#)). We compared the PMs measured by Hipparcos and Gaia DR3 with predictions of our model (which accounts for motion of the photo-centre in both orbits) and found them to be in reasonable agreement.

Figure 2 places the components of HIP 86286 on the $(M_V, V - K$

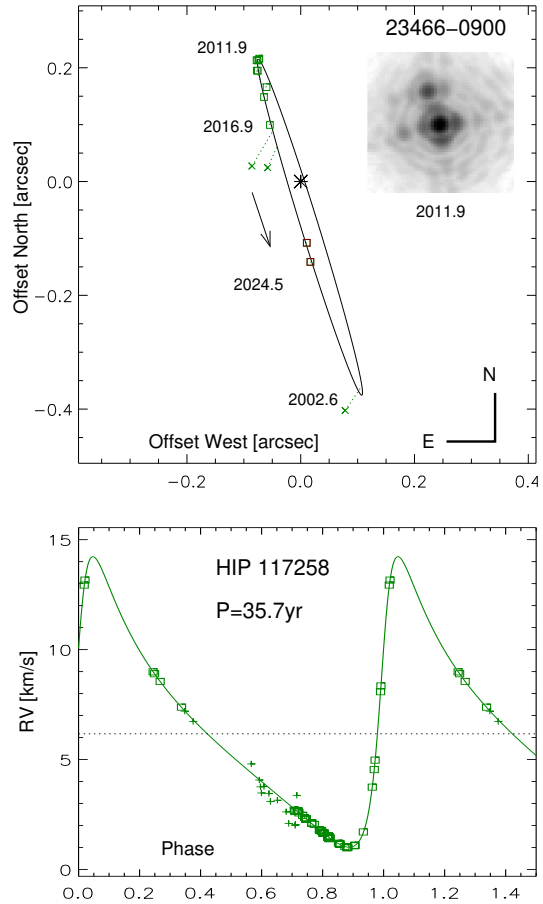


Figure 3. Orbit of HIP 117258 in the plane of the sky (top) and the RV curve (bottom; CORAVEL data are plotted as pluses). The insert shows image of this pair in the K band from ([Tokovinin et al. 2012](#)).

K) colour-magnitude diagram. Comparison with the PARSEC isochrones ([Bressan et al. 2012](#)) indicates an age about 5 Gyr. The effective temperatures and colours of all three stars are similar, but the component A is substantially brighter than C and B. Star A evolves rapidly: a minor variation of its mass or age results in a large change of the temperature and colour; the two selected isochrones bracket the actual $V - K$ colour at $1.22 M_{\odot}$ mass, slightly less than $1.28 M_{\odot}$ derived by the approximate Montalto formula.

The similarity of the inclinations and nodes of the inner and outer orbits is notable. The mutual inclination between the orbits is 9° , their eccentricities are moderate, and the ratio of the periods is only 8.2. This triple system resembles a class of hierarchies with relatively well-aligned and quasi-circular orbits. For example, HIP 85209 (WDS J17247+3802) is a quadruple system with estimated outer period of ~ 500 yr, intermediate period of 38 yr, and the inner (also resolved) subsystem with a 1.23 yr period; its components have slightly sub-solar masses, and the two inner orbits are oriented nearly edge-on ([Tokovinin et al. 2019](#)).

4 HIP 117258, A HIDDEN TRIPLE SYSTEM

This bright ($V = 7.228$ mag) solar-type system, HIP 117258 (HD 223084, WDS J23466–0900, LTT 9700, F9V), was identified as Hipparcos accelerating binary by [Makarov & Kaplan \(2005\)](#). It was resolved in 2002 by [Lloyd \(2002\)](#) with adaptive optics at the 3-

Table 4. Orbit and Astrometry of HIP 117258

| Element | Value |
|--|--------------------------------|
| P (yr) | 35.71 ± 0.38 |
| T (JY) | 2008.980 ± 0.027 |
| e | 0.595 ± 0.004 |
| a (″) | 0.3701 |
| Ω_A (deg) | 17.67 ± 0.20 |
| ω_A (deg) | 291.65 ± 0.09 |
| i (deg) | 87.55 ± 0.10 |
| K_1 (km s $^{-1}$) | 6.608 |
| V_0 (km s $^{-1}$) | 6.167 ± 0.030 |
| RA, Decl. (J2000) | $23:46:34.1097, -08:59:48.962$ |
| μ_α^*, μ_δ (mas yr $^{-1}$) | $183.66, -68.08$ |
| Parallax (mas) | 26.922 ± 0.085 |

m Lick telescope and, independently, in 2011 and 2012 using the NICI adaptive optics instrument at Gemini-S (Tokovinin et al. 2012, 2013). The orbital motion of this pair was followed during 2013–2024 by the speckle camera at SOAR. The star was also monitored in RV in search of exoplanets by two teams (Fischer et al. 2014; Barbato et al. 2023). A substantial RV variation indicated a stellar-mass companion, rather than a planet, and Barbato et al. determined a spectroscopic orbit with a period of 36.41 yr; their RV data span from 1985 to 2021 and cover one full orbital cycle. They do not mention direct resolutions.

Taken together, the position measurements and the precise RVs constrain the orbit of this pair, seen edge-on, quite well (Fig. 3). The relative photometry of the resolved binary ($\Delta K = 1.86 \pm 0.1$ mag, $\Delta H = 2.19 \pm 0.1$ mag, $\Delta I = 3.23 \pm 0.3$ mag) indicates that the secondary companion B is fainter and redder than the main star A. The IR photometry suggests that it should have a mass around $0.65 M_\odot$, assuming that star A has a mass of $1.1 M_\odot$. However, the predicted $\Delta I = 2.95$ mag is smaller than measured. Furthermore, the RV amplitude and inclination imply a companion of $0.95 M_\odot$; the large companion mass is also confirmed by the measured acceleration. If the companion were a main-sequence star with such mass, it would be much brighter (estimated $\Delta K = 0.52$ mag and $\Delta I = 0.72$ mag), contradicting the observations; on the other hand, a white dwarf would be too faint for imaging detection.

The tension is resolved by assuming that companion B is a close pair of low-mass M-type dwarfs. The fitted triple-star model uses relative positions, RVs, Hipparcos and Gaia astrometry, combined photometry, and differential photometry in the I and K bands. The orbital elements in Table 4 result from this model, and their errors are estimated by MCMC. Zero extinction is adopted and verified. Parameters of the stars are listed in Table 5. The modeled magnitude differences between B and A in the I , H , and K bands match the actual differential photometry within errors. The data place no strong constraints on the individual masses of Ba and Bb (only on their sum), and a pair of equal $0.47 M_\odot$ stars would match observations as well.

In our solution this is constrained by assuming that the components are red dwarfs, and their masses are computed from absolute magnitudes M_{K_s} using the 5th order polynomial from Table 6 of Mann et al. (2019) for solar metallicity. The mass of the primary is computed with the same Montalto’s formula as for all three stars in the first example. Our dynamical parallax, 26.922 mas, agrees with the Gaia DR3 parallax of 27.029 ± 0.081 mas. Naturally, the mass sum computed from the orbit with the Gaia parallax is also larger than $1.75 M_\odot$ expected if it were a simple binary; conversely, enforc-

Table 5. Stellar Parameters and Photometry of HIP 117258

| Parameter | A | Ba | Bb | Ba+Bb | A+B |
|--------------------------|-------|--------|--------|--------|-------------|
| Mass (M_\odot) | 1.10 | 0.53 | 0.42 | 0.95 | 2.05 |
| Radius (R_\odot) | 1.05 | 0.53 | 0.42 | ... | ... |
| T_{eff} (K) | 6173 | 3723 | 3497 | ... | ... |
| L (L_\odot) | 1.44 | 0.049 | 0.024 | ... | ... |
| $\log g$ (cm s $^{-2}$) | 4.440 | 4.708 | 4.809 | ... | ... |
| Sp. Type | F8V | M0.9V | M2.5V | ... | ... |
| B (mag) | 7.764 | 13.760 | 14.921 | 13.440 | 7.76 (7.78) |
| V (mag) | 7.238 | 12.293 | 13.399 | 11.958 | 7.24 (7.23) |
| I_C (mag) | 6.636 | 10.304 | 11.088 | 9.874 | 6.636 (...) |
| J (mag) | 6.224 | 9.149 | 9.795 | 8.672 | 6.12 (6.14) |
| H (mag) | 6.000 | 8.534 | 9.207 | 8.067 | 5.85 (5.86) |
| K_s (mag) | 5.939 | 8.313 | 8.962 | 7.837 | 5.77 (5.75) |
| G (mag) | 7.096 | 11.491 | 12.376 | 11.093 | 7.10 (7.07) |
| G_{BP} (mag) | 7.408 | 12.555 | 13.669 | 12.222 | 7.40 (7.39) |
| G_{RP} (mag) | 6.711 | 10.492 | 11.275 | 10.062 | 6.66 (6.64) |

Table 6. Positions and Residuals of HIP 117258

| Date (JY) | θ_{2000} (deg) | (O-C) $_\theta$ (deg) | σ_θ (deg) | ρ (mas) | (O-C) $_\rho$ (mas) | σ_ρ (mas) |
|-----------|-----------------------|-----------------------|-----------------------|--------------|---------------------|---------------------|
| 2002.5877 | 191.0 | -5.7 | 999.9 | 410.0 | 34.8 | 999.9 |
| 2011.8483 | 18.9 | -0.0 | 2.0 | 227.0 | 1.1 | 5.0 |
| 2011.8483 | 18.6 | -0.3 | 2.0 | 228.0 | 2.1 | 5.0 |
| 2012.8285 | 19.7 | -0.1 | 2.0 | 226.0 | 0.9 | 5.0 |
| 2012.8285 | 20.0 | 0.2 | 2.0 | 227.0 | 1.9 | 5.0 |
| 2013.7347 | 21.2 | 0.5 | 1.0 | 208.8 | -4.0 | 5.0 |
| 2014.7613 | 21.6 | -0.3 | 1.0 | 209.7 | 19.5 | 50.0 |
| 2014.8543 | 19.9 | -2.1 | 5.0 | 176.4 | -11.5 | 50.0 |
| 2015.7361 | 23.5 | 0.1 | 1.0 | 161.9 | -1.6 | 5.0 |
| 2016.9568 | 28.6 | 2.4 | 5.0 | 113.2 | -12.2 | 50.0 |
| 2017.6802 | 72.3 | 43.4 | 999.9 | 89.9 | -11.6 | 999.9 |
| 2018.4856 | 67.2 | 33.1 | 999.9 | 63.1 | -11.3 | 999.9 |
| 2023.4180 | 185.6 | 0.9 | 1.0 | 108.2 | -0.2 | 5.0 |
| 2024.4666 | 186.9 | -1.1 | 1.0 | 142.3 | -1.5 | 5.0 |

ing such a small mass sum implies a dynamical parallax of 28.4 mas incompatible with Gaia.

The positions and residuals are listed in Table 6. The inaccurate position from Lloyd (2002) is not used, but with the angle changed by 180° , it fits the orbit approximately. We also ignore the tentative measurements at SOAR in 2017.7 and 2018.5, obtained without reference stars; the pair was not resolved at SOAR from 2018.7 till 2022.4 and opened up in 2023, after passing through a conjunction. We do not reproduce here the published RVs and their errors, available in the cited papers. A slight zero-point correction was determined for the CORAVEL RVs from Barbato et al. (2023), and 2.362 km s $^{-1}$ was added to the RVs from Fischer et al. (2014), so our systemic velocity refers to the CORALIE system.

The centre-of-mass PM of the system determined by our model is $(183.66, -68.08)$ mas yr $^{-1}$. It differs substantially from the mean PM derived by Brandt (2021), $(181.57, -74.67)$ mas yr $^{-1}$, because the orbital period is longer than 24.75 yrs elapsed between Hipparcos and Gaia DR3 epochs (the companion was at opposite ends of its orbit in those epochs). Our model predicts the photo-centre motion of $(186.95, -54.28)$ mas yr $^{-1}$ at the Gaia DR3 epoch and agrees with the measured PM of $(187.78, -54.37)$ mas yr $^{-1}$ reasonably well.

The triple-star model implies a magnitude difference of 5 mag between A and Ba in the V band, so the 1% contribution of light from Ba to the combined spectrum is not detectable without additional effort. If B is a close pair of M dwarfs with a period of a few days, the RVs of Ba and Bb vary with large amplitudes. Blending of their weak lines with the lines of A could cause a subtle variation of the measured RVs. Yet, the residuals of RVs measured with CORALIE (the most precise data set) are in agreement with the declared errors. The RV perturbation would be less if Ba were a fast rotator with broad and shallow lines or if Ba and Bb were equal and moved in opposite sense, canceling potential blending of their lines with A.

A similar solar-type triple system with a dim yet massive companion on a 26 yr orbit is κ For or HIP 11072 (Fekel et al. 2018). The reality of the close inner pair is confirmed by the X-ray and radio detections, attributed to active chromospheres of the low-mass dwarfs with fast rotation. Weak lines of the secondaries were tentatively detected in the combined spectrum after subtracting the main star (Tokovinin 2012), suggesting an orbital period of 3.7 days. In contrast, no X-rays from HIP 117258 were reported, probably because it is 1.6 times further away than HIP 11072.

To search for weak lines of the inner pair, a high-resolution optical spectrum of HIP 117258 was taken using the CHIRON spectrograph at the 1.5-m telescope in Chile (Tokovinin et al. 2013) on JD 2,460,543.7706. Its cross-correlation with the solar template reveals only one strong dip with a heliocentric RV of 6.115 km s^{-1} and a width corresponding to the projected rotation velocity of 5.1 km s^{-1} . No secondary dips with amplitude above 1% are found. The lithium 6707Å line with an equivalent width of $50 \pm 5 \text{ mÅ}$ is present. The projected rotation velocity corresponds to a rotation period of 10 days if the inclination is close to 90° , or shorter if the axis is inclined. The RV agrees with the orbit (residual $+0.16 \text{ km s}^{-1}$).

A close pair in the secondary component of HIP 117258 could manifest itself by flux modulation due to eclipses or starspots. However, the light curves recorded by the TESS satellite (Ricker et al. 2014) do not reveal any eclipses. Instead, an irregular modulation with a period of 5 or 10 days and an amplitude of $\sim 0.3\%$ is seen. Considering the small contribution of Ba and Bb to the total flux, this modulation is likely caused by starspots on the main star. No strong flares were noted.

Summarizing, the case for HIP 117258 hosting a triple system is strong, and there are no other viable explanations for the large mass of the dim secondary. The evidence, however, is indirect. Our efforts to find additional clues from spectroscopy or space photometry have not produced any tangible results.

5 SUMMARY

We presented here the method where diverse data available on each stellar system are fitted by a model comprising orbital elements, physical parameters of the stars, and distance (dynamical parallax). The assumption that stars obey empirical relations between mass, effective temperature, and radius is built into the model and checked by examination of the fitted parameters.

The method is applied here to two nearby triple systems, establishing new facts on their structure and parameters. The first one, HIP 86286, is unusual because its two faint resolved companions are located at comparable separations. We determine the orbital periods of 35 and 287 years and show that the orbits are approximately coplanar. This system therefore has a planetary-type architecture. The other system, HIP 117258, has been known until now as a simple binary. We determine its accurate 36-yr orbit, revealing that

the secondary companion is over-massive. The secondary should be a close pair of M-type dwarfs with yet unknown period. So, HIP 117258 joins the group of triple solar-type stars with dim yet massive secondary companions which are themselves close pairs, similar to κ For (HIP 11072).

The two triple systems studied here are problematic for Gaia, for different reasons (complicated source structure and insufficient time coverage), but the combination of Gaia with ground-based data has a great power.

Our findings contribute to the database on hierarchical systems (Tokovinin 2018), albeit by a small increment, and advance the still incomplete knowledge of multiple-star populations in the solar neighborhood.

ACKNOWLEDGMENTS

We thank the Referee for useful comments that improved the paper. This work used the SIMBAD service operated by Centre des Données Stellaires (Strasbourg, France), bibliographic references from the Astrophysics Data System maintained by SAO/NASA, and the Washington Double Star Catalog maintained at USNO. We thank R. Matson for retrieving the historic micrometer measurements. Modern position measurements used here were obtained at the Southern Astrophysical Research telescope. This work has made use of data from the European Space Agency (ESA) mission Gaia (<https://www.cosmos.esa.int/gaia>), processed by the Gaia Data Processing and Analysis Consortium (DPAC, <https://www.cosmos.esa.int/web/gaia/dpac/consortium>).

DATA AVAILABILITY

Only published data were used in this research.

REFERENCES

- Baraffe, I., Homeier, D., Allard, F., Chabrier, G. 2015, *A&A*, 577, A42
 Barbato, D., Ségransan, D., Udry, S. et al. 2023, *A&A*, 674, 114
 Brandt, T. D. 2021, *ApJS*, 254, 42
 Bressan, A., Marigo, P., Girardi, L., et al. 2012, *MNRAS*, 427, 127
 Claret, A. 2018, *A&A*, 618, A20
 Chulkov, D., Malkov, O. 2022, *MNRAS*, 517, 2925
 Fekel, F. C., Willmarth, D. W., Abt, H. A., Pourbaix, D. 2018, *AJ*, 156, 117
 Fischer, D. A., Marcy, G. W., Spronck, J. P. 2014, *ApJS*, 210, 5
 Foreman-Mackey, D., Hogg, D. W., Lang, D., Goodman, J. 2013, *PASP*, 125, 306
 Gaia Collaboration, Brown, A. G. A., Vallenari, A., et al. 2021, *A&A*, 649, A1
 Gaia Collaboration, Arenou, F., Babusiaux, C., et al. 2023, *A&A*, 674, A34
 Høg, E., Fabricius, C., Makarov, V. V., et al. 2000, *A&A*, 357, 367
 Lloyd, J. P. The detection and characterization of low mass companions to sun-like stars. Thesis (PhD). Univ. of California (Berkeley), Source DAI-B 64/02, p. 764, Aug 2003, 270 pp.
 Makarov, V. V., Kaplan, G. H., 2005, *AJ*, 129, 2420
 Mann, A. W., Dupuy, T., Kraus, A. L., et al. 2019, *ApJ*, 775, 871, 63
 Montalto, M., Piotto, G., Marrese, P. M. et al. 2021, *A&A*, 653, A98
 Moya, A., Zuccarino, F., Chaplin, W. J., Davies, G. R. 2018, *ApJS*, 237, 21
 Peca, M. J. & Mamajek, E. E. 2013, *ApJS*, 208, A9
 Ricker, G. R., Winn, J. N., Vanderspek, R., et al. 2014, in Society of Photo-Optical Instrumentation Engineers (SPIE) Conference Series, Vol. 9143, Space Telescopes and Instrumentation 2014: Optical, Infrared, and Millimeter Wave, 914320
 Stassun, K. G., Oelkers, R. J., Paegert, M. et al. 2019, *AJ*, 158, 138

- Tokovinin, A. 2012, *AJ*, 145, 76
Tokovinin, A. 2017, *ORBIT3: Orbits of Triple Stars*, Zenodo, doi:
10.5281/zenodo.321854
Tokovinin, A. 2018, *ApJS*, 235, 6
Tokovinin, A., Hartung, M., Hayward, Th. L., Makarov, V. V. 2021, *AJ*, 144,
7
Tokovinin, A., Hartung, M., Hayward, Th. L. 2013, *AJ*, 146, 8
Tokovinin, A., Everett, M.E., Horch, E.P., Torres, G., Latham, D.W. 2019,
AJ, 158, 167
Tokovinin, A., Fischer, D. A., Bonati, M., et al. 2013, *PASP*, 125, 1336
Tokovinin, A., Mason, B.D., Hartkopf, W.I., Mendez, R.A., Horch, E.P. 2018,
AJ, 155, 235
Tokovinin, A., Mason, B.D., Mendez, R.A., Costa, E. 2022, *AJ*, 164, 58
van Leeuwen, F. 2007, *A&A*, 474, 653

This paper has been typeset from a $\text{\TeX}/\text{\LaTeX}$ file prepared by the author.